Proceedings of ICONE15:
15th International Conference on Nuclear Engineering
April 22-26, 2007, Nagoya, Japan

ICONE-15-10291

SOLVING POROUS MEDIA FLOW FOR LWR COMPONENTS

Miettinen Jaakko
VTT, P.O.Box 1600
FIN-02044 VTT, Finland
Phone:+358 20 722 5032
Fax:+358 20 722 5000
jaakko.miettinen@vtt.fi

Ilvonen Mikko
VTT, P.O.Box 1600
FIN-02044 VTT, Finland
Phone:+358 20 722 5054
Fax: :+358 20 722 5000
mikko.Ivonen@vtt.fi

Keywords: 3D-flow, porous media solution.

ABSTRACT

A porous media solution PORFLO has been developed for the 3-dimensional two-phase flow by describing the process facility with Cartesian or cylindrical coordinates. The local porosity fraction is applied for distinguishing the fluid filled volumes from the solid structures. The solid structure contribute the two-phase flow through the wall friction, flow area and heat transfer. The solid structure may contain heat input by steam generator tubes, steam condenser tubes or internal heating of solid particles. The first phase of the model development has included the modelling for these applications.

The thermohydraulic solution is based on 5-equation approach, where the conservation equations are solved for the liquid and gas mass, mixture momentum, liquid and gas energy.

The first application for the model was the calculation of the particle bed dryout cooling experiments. In experiments the core debris coolability on the containment pedestal floor has been studied to verify the severe accident management strategy adapted in Olkiluoto BWRs. The decay power heating of the real core debris is generated by electrical resistance heaters.

The second application is related to passive safety systems of BWR plants. In the isolation condenser the steam from the reactor vessel is flows through the heat transfer tubes. The tube bundle has been submerged into the cold water pool. After a short heating period vigorous boiling takes place in the poll creating strong two-phase circulation. The 3-dimensional flow two-phase flow circulation was calculated for the pool. The work was a part of the new nuclear plant evaluation concept for the nuclear power plant candidates for Finland. After the EPR plant was selected, the more detailed analyses were not continued. The steam condensation inside the heat transfer tube may be modelled by using an 1-dimensional model.

As a future application the characteristics of the horizontal steam generator is studied. The primary fluid flow inside the heat transfer tubes creates the heat transfer boundary condition. Some scattered data from the local void fractions exists for the facility and at least the shape of the two-phase level during the steady state operation has been recorded.

The present PORFLO model is based on the drift-flux model with five conservation equations, when the complete two fluid model includes six conservation equations, mass, momentum and energy equations for both phases. The question is, would the drift flux model be too limited for the 3D two-phase flow? The author's opinion is that the approach gives just for the large facilities a good modelling possibility. The drift-flux formalism with two input parameters is a clear-cut formulation, and rather much experimental data has been formulated by using the drift-flux formalism. In the three reference facility of the PORFLO application the local void fractions are in the range of 0 to 0.4, where liquid is continuous phase and vapour exists in the form of bubbles. For this flow regime the vapour phase does not transmit any momentum. Additionally the drift flux model is capable for modelling the sharp void fraction gradient at the two-phase level.

The three applications demonstrate that the porous media approach based on the drift-flux model is applicable for modelling the real process facilities, where the water level exists and the two-phase flow patterns is generated mainly by the local gravitational pressure differences. The particle bed dryout experiment, the BWR isolation condenser and the horizontal VVER steam generator are examples of such facilities.

1. INTRODUCTION

In the first PORFLO applications the modelling of the two-phase mixture in the large process facilities have been studied, where the heat input inside the liquid pool evaporates liquid and the generated vapour tends to rise upwards and separate from the liquid on the water level. The heat inputting section includes heat transfer tubes or internally heated particles submerged into the liquid. Only 30 to 50 % from the local volume may be available for the fluid flow in this sections and the solid material created additional frictional pressure drop in the circulating flow. A part on the facility may be fully open space for the fluid flow and there easily strong turbulent circulation may exists in the two-phase mixture. The water level separates the single phase steam flow from the two-phase mixture, where the liquid is the continuous phase and vapour exists mainly as bubbles. Additionally isolating walls may exists for controlling the coolant circulation

The first application with the PORFLO model was related to the dryout testing facility of the internally heated particle bed.

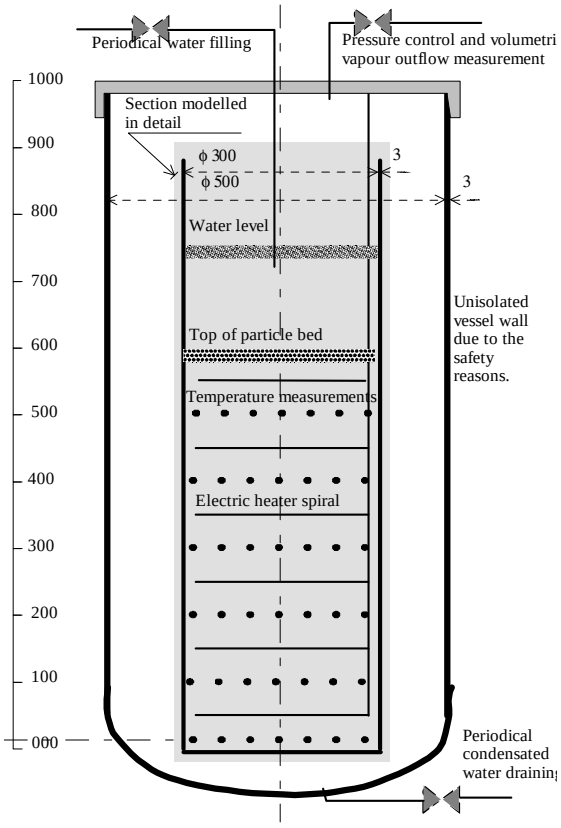

Figure 1. STYX particle bed dryout experimental facility at VTT

A facility has been constructed at VTT to measure dryout heat flux in a heterogeneous particle bed, Figure 1. The inner cylindrical vessel is enclosed into the pressure vessel, making experiments at 1 – 7 bar pressure possible, The particle bed is immersed into water and water level is maintained constant. The electrical heating coils are located on 6 elevation in the bed. When the heating power is increased over a threshold value, the bottom of the bed is overheated, in spite the water above the bed top. The dryout mechanism is caused by the counter-current-flow-limitation, when rising vapor presents the water falling down and cooling lower parts of the bed.

The experimental bed dimensions are 0.3 m in diameter and 0.6 m in height, with a mixture of 0.1 to 10 mm particles. The facility has a pressure range from atmospheric to 7 bar. The bed is heated by spirals of a resistance band. A series of experiments have been carried out, and the analysis with several multidimensional analysis tools is in progress.

The PORFLO code could predict the general parameters trends in the facility. The dryout-power and system power can be predicted properly when the drift flux parameters are adjusted giving the CCFL conditions at the power level of the experiment. The adjustment of the analysis model by using the drift flux parameters was considered so special, however, that before more final analyses and final conclusions other 2D analysis tools for the analysis of experimental data systematically. After these analyses the proper criteria for the PORFLO drift flux model are can be formulated.

The isolation condenser is a passive safety component related to the BWR 90+ reactor concept (Haukeland, 2000). Its role is heat removal from the reactor system during transient conditions and reactor shutdown. The main component of the condenser are depicted in Fig. 2. The inlet collector of the condenser is connected into the upper plenum. During shutdown steam flows into the collector and enters the heat exchanger tubes. The tubes are submerged into the cold water pool and steam condenses on the tube inside. The condensate flows from the outlet collector to the reactor downcomer. By controlling the outlet flow rate the water level in the outlet collector is regulated. By low water level the condenser is functioning with full effect. When the water level is increased, the condensation efficiency is reduced.

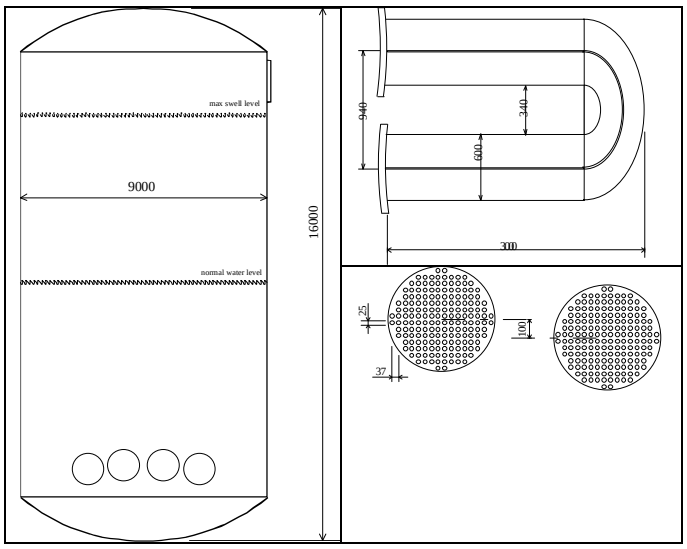

Figure 2 Main component of the isolation condenser, the cylindrical pool filled with cold water (left), the tube bundle (right top) and its tubes (right bottom).

The rated power of the condenser is 145 MW and outside surface area for 176 tubes with 25 mm O.D. is 83 m^2. The heat flux rate 1.75 MW/m^2 means 0.8 m^3/s boiling and immediate condensation on the tube shell side.

In modelling of the condenser the most essential section is the heat transfer tubes, both their primary side and secondary side. On the primary side hot steam is condensed on the walls, and the conducted through the heat transfer tubes creates the heat source for the secondary water pool. The void fraction from boiling creates a massive circulation in the pool.

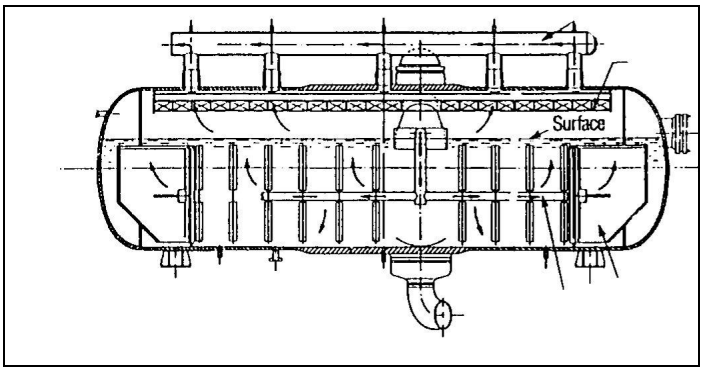

Figure 3 Horizontal steam generator used in the Loviisa VVER-440 plant.

In the horizontal steam generator of VVER-reactors the heat transfer tubes having high pressure single phase water inside are submerged into the secondary water pool. The heat transported by the primary tubing creates boiling on the outer surface of the tubes, and consequently a strong circulation of the secondary water due to a gravitational effect of the void generation. In this steam generator type all the phase separation is based on the gravitation separation in the secondary water pool. In the vertical steam generation the gravitational phase separation is strengthened by the steam generator wide circulation between the riser and downcomer areas.

In Figure 3 the Loviisa steam generator is depicted. If the two mixture conditions on the secondary side can be simulated including the void fraction and temperature distribution, the plant characteristics may be studied more accurately. The heat transport by the primary tubes has to be described with a sufficient accuracy for the primary convection and heat transfer through the tubes. The operational pressure of the steam generator is 45 bar, the flow through the primary tubes 1400 kg/s and vapour generation rate 130 kg/s.

The secondary side of an entire steam generator can be analyzed 3-dimensionally with a reasonable amount of secondary nodes in a porosity model. The cross section described by 20 x 20 nodes, and axial length by 50 nodes results as 20000 nodes, where each of them includes heat transfer tube structures and free volume for fluid circulation. The porosity model is just proprietary for the described process facilities, where the gravitational forces are the main reason for the two-phase circulation and the void fraction inside the water pool is reasonable low.

2. TWO-PHASE SOLUTION FOR THE TWO-PHASE WATER POOL

2.1 Basic conservation equations

In the porous media model the most important two-phase flow solution takes place in the gravitationally circulating water pool. The model solves three-dimensional the liquid – vapour conservation equations. The porosity means that only a part of the volume is available for the fluid. The wall friction between the fluid and solid material is essential. The solid material may be the source of the liquid heating and the vapour generation as well.

The existence of tubes or internally heated particles in individual volumes is considered through the porosity, which for the particle bed is typically 30-40 % from the total volume, and for the steam generator or condenser it depends on pitch between heat transfer tubes. In the isolation condenser the heat transfer tubes fill only a small fraction on the water filled volume. In the steam generator the heat transfer tubes occupy the major part of the water filled section. Above the tubes a layer of free circulating water exists making possible of phase separation. In addition to that the gaps exists at ends and on the sides between the tube bundle and cylindrical tank.

The thermohydraulic solution is based on 5-equation approach, where the conservation equations are solved for the liquid and vapour mass, mixture momentum, and liquid and gas energy. The friction is applied only between the heaters. The heat transfer model between the tubes and fluid includes convection into liquid, boiling, convection into gas, cooling of gas by existing liquid, flashing due to liquid superheat and condensation due to liquid subcooling. The system pressure is used for gas densities and saturation temperature for stabilising the solution, but the saturation temperature includes the gravitational pressure effect (not the dynamic pressure effect). The phase separation is solved using the drift flux model. In the drift-flux model the pressure-velocity solution is needed only for the average mixture velocity, not for each phase separately.

The mass conservation for the 3D two-phase model is written for the gas phase through:

$$\frac{\partial(\alpha\rho_g)}{\partial t}+\frac{\partial(\alpha\rho_g u_g)}{\partial x}+\frac{\partial(\alpha\rho_g v_g)}{\partial y}+\frac{\partial(\alpha\rho_g w_g)}{\partial z}=-\gamma \quad (1)$$

and for the liquid phase through

$$\frac{\partial((1-\alpha)\rho_l)}{\partial t}+\frac{\partial((1-\alpha)\rho_l u_l)}{\partial x}+\frac{\partial((1-\alpha)\rho_l v_l)}{\partial y}+\frac{\partial((1-\alpha)\rho_l w_l)}{\partial z}=+\gamma \quad (2)$$

For the solution the equations are summed into the mixture mass conservation equation and the resulting mixture mass conservation equation reads

$$\frac{\partial(\rho_m)}{\partial t}+\frac{\partial(\rho_m u_m)}{\partial x}+\frac{\partial(\rho_m v_m)}{\partial y}+\frac{\partial(\rho_m w_m)}{\partial z}=-\gamma \quad (3)$$

The local porosity in not included into these equations. It is included into the integral form, where the fluid volume equals with the free volume, and flow area equals with the available flow connection between junctions. In the staggered grid approach the flow velocities are related to the interface between nodes. The time derivative of the density is written by using the time derivative for the pressure, after the enthalpy related part of the density is assumed constant during solution of the pressure-velocity equation.

The momentum conservation for the 3D two-phase model in the primitive form for the mixture in the vertical direction is defined through

$$\frac{\partial(\rho_m w_m)}{\partial t}+\frac{\partial(\rho_m w_m^{\,2})}{\partial x}=-\frac{\partial p}{\partial z}+\frac{\partial p_f}{\partial z} \tag{4}$$

in one horizontal directions through

$$\frac{\partial(\rho_m u_m)}{\partial t}+\frac{\partial(\rho_m u_m^{\,2})}{\partial x}=-\frac{\partial p}{\partial y}+\frac{\partial p_f}{\partial y} \tag{5}$$

$$\frac{\partial(\rho_m v_m)}{\partial t}+\frac{\partial(\rho_m v_m^{\,2})}{\partial x}=-\frac{\partial p}{\partial y}+\frac{\partial p_f}{\partial y} \tag{6}$$

The frictional pressure loss between the solid and fluid may be formulated to give in the vertical direction with the gravitational pressure loss as well in the form

$$\frac{\partial p_f}{\partial z}=-0.5\times(\frac{f}{d_e})\rho_m w_m|w_m|-\rho_m g \tag{7}$$

and in the horizontal x –direction, and in the y-direction is similarly

$$\frac{\partial p_f}{\partial x}=-0.5\times(\frac{f}{d_e})\rho_m u_m|u_m| \tag{8}$$

In the solution of the pressure-velocity equation the momentum equation is discretized and the velocities in the mass conservation equation are replaced by the solutions of the momentum equation. As a result of this replacement the mass conservation equation is reduced to a single pressure solution.

The liquid and gas energy conservation equations are derived from phase enthalpy equations. The primitive forms of the equations is used for the integration, where the enthalpy changes are small. The enthalpy conservation equations are expressed for the gas enthalpy through

$$A\alpha\rho_g\frac{\partial(i_g)}{\partial t}+A\alpha\rho_g u_g\frac{\partial(i_g)}{\partial x}+A\alpha\rho_g v_g\frac{\partial(i_g)}{\partial y}+A\alpha\rho_g v_g\frac{\partial(i_g)}{\partial z}=Aq_{wg}^{'''}+Aq_{lg}^{'''} \tag{9}$$

and for the liquid enthalpy as

$$A(1-\alpha)\rho_l\frac{\partial(i_l)}{\partial t}+A(1-\alpha)\rho_l u_l\frac{\partial(i_l)}{\partial xz}+A(1-\alpha)\rho_l v_l\frac{\partial(i_l)}{\partial xz}+A(1-\alpha)\rho_l v_l\frac{\partial(i_l)}{\partial z}=Aq_{wl}^{'''}+-Aq_{lg}^{'''} \tag{10}$$

2.2 Heat transfer from tubes into the pool

The heat input into the fluid is calculated with the surface heat transfer function from the surface of the heater tubes.

The heat transfer modes between the heaters and fluid include convective heat transfer to liquid (only heating of liquid), boiling heat transfer, if wall temperature is superheated ($T_w > T_{sat}$) (all heat used for liquid evaporation), convective heat transfer to gas (only heating of gas) and condensation of steam into the subcooled wall ($T_w < T_{sat}$). The interphasial heat transfer includes flashing, if liquid is superheated, and condensation, if subcooled liquid is in contact with steam. The wall heat transfer models include the porosity, and consequently it the heat flow from structures approaches zero by the porosity equal to zero (no structure in the volume) and equal to one (volume filled with solid structure).

After dryout the heater walls are in contact to gas and are heating only the gas phase. In the model the contact area with steam is proportional to the void fraction. The heat transfer rate for the unit volume is formulated as

$$q_{wg}^{'''}=h_{wg}^{'''}(T_w-T_g)\alpha\varepsilon(1-\varepsilon) \tag{11}$$

The correlation for the liquid heating read

$$q_{wl}^{'''}=h_{wl}^{'''}(T_w-T_l)(1-\alpha)\varepsilon(1-\varepsilon) \tag{12}$$

The boiling is added into the heat transfer when the solid heater temperature exceeds the saturation temperature. The effect of the void fraction is described by using a nonlinear function. The boiling correlation reads

$$q_{wb}^{'''}=h_{wb}^{'''}\max(T_w-T_s,0)^2(1-\alpha)^{0.3}\varepsilon(1-\varepsilon) \tag{13}$$

The boiling and convection heat transfer is consumed to the evaporation through, if the water subcooling is below the given limit

$$\gamma=\max(30.+T_s-T_l,0)(q_{wb}^{'''}+q_{wl}^{'''})/h_{lg} \tag{14}$$

and the rest is used for the liquid heating. The value 30 is the selected ramp parameter for the incipience of boiling in the present model.

The flashing heat transfer becomes significant, when water is superheated due to hot heaters or hot gas. The flashing term is expressed through

$$q_{l.fla}^{'''}=h_{l,fla}\max(T_l-T_s.0)(1-\alpha)\varepsilon \tag{15}$$

The condensation heat transfer is possible, if steam is in contact with subcooled liquid. By considering all precautions in the heater bundle the formulation may be defined by

$$q_{l.con}^{'''}=h_{l,con}\max(T_s-T_l.0)\varepsilon\alpha(1-\alpha) \tag{16}$$

The mass transfer due to flashing and condensation is defined through

$$\gamma=-q_{l,con}^{'''}/h_{lg}\quad\text{and}\quad\gamma=q_{l,fla}^{'''}/h_{lg} \tag{17}$$

The gas cooling is possible, when liquid contacts superheated gas and the correlation is given through

$$q_{gl}^{'''}=h_{gl}^{'''}\max(T_g-\max(T_l,T_s)\ ,0)\alpha\varepsilon(1-\varepsilon) \tag{18}$$

In most conditions, the accuracy of the critical heat flux (CHF) correlation on the pool side is not essential. If dryout conditions are encountered, however, if insufficient water exists locally in the heater section. This situation is encountered in specially in the particle bed dryout

experiment. By applying the Zuber CHF correlation the following form for the critical heat flux may be derived

$$\frac{q''_{CHF}}{h_{fg}\rho_v} = 0.131\left(\frac{\sigma(\rho_l-\rho_v)g}{\rho_v^2}\right)^{0.25}(1-\alpha) \quad (19)$$

When the heat transfer coefficients are expressed by using the porous media formalism, the heat structures are not considered through the heat source per tube surface area. The coolant volume is related to the heater area through the equivalent diameter defined through

$$d_{eq} = \frac{4V_{fl}}{A_w} \quad (20)$$

and with this relation the surface heat flux is converted into the volumetric heat flux.

The volumetric heat transfer coefficients are derived from pool boiling correlations. The order of magnitude for the selected coefficients are presented in Table 1.

Table 1. Heat transfer coefficient for different heat transfer modes.

Mode		Basis
Liquid heating	h_{wl}	Convection, Dittus-Boelter
Gas heating	h_{wg}	Convection, Dittus-Boelter
Boiling	h_{wb}	Boiling heat transfer, Thom
Condensation	h_{cn}	User constant
Flashing	h_{fl}	No liquid superheat

In the further model testing the refinement of the wall heat transfer model may expected. One example is the CHF –correlation. The deficiency in many correlations is that they are valid only the single tube or for the flow along the tube bundle. The correlation of Kezios, discussed in (Tong, 1972) is mentioned as a useful correlation for the cross flow conditions in the tube bundle and it is written through

$$q''_{CHF} = 7.37\times10^3\left(\frac{G}{3600}\right)^{0.53}\Delta T_{sub}^{0.77}X_t^{-0.4} \quad (21)$$

where the British units have to be applied. Thus T as F, G as lb/hr/ft^2 and q as Btu/hr/ ft^2. The X_t coefficient defines the ratio between the rod pitch and rod diameter. The correlation can be considered representative only for the DNB –type of CHF. Because the shortage of water should be considered as well, the correlation could be combined together with that of extended Zuber.

2.4 Phase separation by using the drift-flux model

The drift flux formalism, which is known as the Zuber-Findlay drift-flux model is applied. It defines the steam velocity as a function of the total mixture velocity and two empirical parameters through

$$u_g = C_o(\alpha)\, j_m + V_{gj}(\alpha) \quad (22)$$

The fitting parameter C_o is called the distribution parameter and V_{gj} the drift flux velocity. The drift-flux parameters are defined by the user, and for the full scale pool calculation the values C_o = 1.2 and V_{gj} = 0.90 m/s have been used.

By applying this formula the volumetric gas flow is given by

$$J_g = \alpha\,(C_o J_m + AV_{gj}) = \alpha\,(C_o(J_g+J_l)+AV_{gj}) \quad (23)$$

By extracting the void fraction from (22) an expression for the void fraction in the quasi-stationary flow is achieved

$$\alpha = \frac{J_g}{C_o(J_g+J_l)+AV_{gj}} \quad (24)$$

The drift flux model can be modified for the relative velocity between phases us quasi-stationary flow through

$$\Delta u = u_g - u_l = \frac{(C_o-1)j_m + V_{gj}}{(1-\alpha)} \quad (25)$$

In the literature study described in the beginning no applicable data was found, which could be used to match the phase separation with the experimental data. But the work will be continued in this area.

But in addition to the heat transfer and frictional loss, the shell side conditions are strongly affected by the phase separation as well. The phase separation model in the computer codes is typically so tightly coupled into the conservation equations for the mass, momentum and energy, that alternative void fraction prediction formulas would be welcome at least for the model validation.

One example the void fraction model from (Schaffrath ,1999) can be mentioned. The void fraction in the cross flow conditions inside the tube bundle is expressed as a function of the dimensionless gas velocity

$$j_g^* = \frac{\rho_g^{1/2} j_g}{\sqrt{gD(\rho_l-\rho_g)}} \quad (26)$$

where j_g means the dimensioned superficial velocity of gas (m/s) and D the tube diameter. By using this dimensionless superficial velocity the local void fraction is expressed through

$$\alpha = 1 - \frac{1}{\sqrt{1+C_1 j_g^* + C_2 j_g^{*2}}} \quad (27)$$

For the in-lined bundle with P/D = 1.3 –1.75, the coefficient C_1 = 35. The coefficient C_2 = 1 when $j_g^* < 0.2$ and C_2 = 30 when $j_g^* > 0.2$. For the staggered bundle, with P/D = 1.3 C_2 = 80 and with P/D=1.75 C_2 = 220. The result proves that the phase separation conditions are strongly varying as a function of the bundle pitch and staggering of tube rows. The result are not directly giving the drift-flux parameters. But the drift-flux model may fitted giving the same result.

2.4 Friction in the tube filled nodes

No friction exists in the sections not filled with tubes. In the tube bundle area the most essential friction is needed for the cross flow conditions. If the tube bundle is tight, one possibility is using of a porous media friction model. In (Feng, 2001) tube bundle friction applicable for the secondary sides of the steam generators is described by using the Darcy-Forcheimer drag force expressed through

$$F_{DF} = \frac{\mu u_f}{\kappa} + \frac{F\rho u_f^2}{\sqrt{\kappa}} \quad (28)$$

The permeability κ and the inertial coefficient F are defined as a function of the porosity ε and tube diameter as

$$\kappa = \frac{\varepsilon^3 d^2}{150(1-\varepsilon)^2}, \qquad F = \frac{1.75}{\sqrt{150}\varepsilon^{1.5}} \quad (29)$$

In (Dowlati, 1992) a cross flow friction loss for the bundle has been derived by combining the friction loss coefficient for a single tube and summation effect resulting from the several tube layers. The single tube cross flow friction correlation is expressed through the general form

$$f = A\,\mathrm{Re}^{-n} \tag{30}$$

For the value pairs A and n a good match into different experiments: A=3.29 / n=0.18 ; : A=7.76 / n=0.28 ; : A=0.4 / n=0.06 ; A=45. / n=0.53 . The superposition principle combining together the effect of several tube rows is expressed through

$$\Delta p = \frac{N\, f\,(G(1-x))^2}{2\,\rho_l} \tag{31}$$

Where N= number of pipe rows. In the work the pitch to diameter radio P/D = 1.3 … 1.75 were found well presented by the correlation for the mass flux range 100 to 800 kg/m^2/s, mixture quality 0 to 0.15 and liquid Reynolds number 700 to 15000.

In the present version the bundle friction is given by the user through a constant parameter, and when the user parameter 0.02 is selected, it directly used as f = 0.02.

3. ONE-DIMENSIONAL TWO-PHASE SOLUTION FOR THE HEAT TRANSFER TUBES

3.1 conservation equations for the heat transfer tubes

The physical characteristics of the condensation process inside the heat transfer tubes was not modelled in the first version of the model. But for more accurate heat transfer the condensation profile in the tubes has to be derived. In the same way the local heat transfer from the steam generator tubes is based on the integration along the heat transfer tube length.

Inside the heat transfer tubes the one-dimensional conservation equations is solved for the two-phase mixture. The condensed steam may contain noncondensable gas as well. The phase separation inside the tube can be expressed with the drift-flux formalism as well.

The one-dimensional mixture mass conservation equation reads

$$\frac{\partial(A\rho_m)}{\partial t} + \frac{\partial(W_m)}{\partial z} = As_l + As_g \tag{32}$$

and the mixture momentum conservation equation

$$\frac{\partial}{\partial t}W_m + \frac{\partial}{\partial z}\frac{1}{A}\frac{W_m^2}{\rho_m} = -A\frac{\partial p}{\partial z} - A\left(\frac{\partial p}{\partial z}\right)_f - A\rho_m g\cos\theta \tag{33}$$

The gas enthalpy conservation equation is defined through

$$\frac{\partial}{\partial t}(A\rho_g h_g) + \frac{\partial}{\partial z}(W_g h_g) - A\alpha\frac{\partial p}{\partial t} = h_{g,i}As_g + Q_g \tag{34}$$

and the liquid enthalpy conservation equation

$$\frac{\partial}{\partial t}(A\rho_l h_l) + \frac{\partial}{\partial z}(W_l h_l) - A(1-\alpha)\frac{\partial p}{\partial t} = h_{l,i}As_l + Q_l \tag{35}$$

The non-condensable gas content in the steam may be defined as well, and by this concentration is weakening of the heat exchanger function.

3.2 Phase separation in the condensing horizontal tubes

The phase separation outside the heat transfer tubes is based on the drift-flux model with large tube diameter parameters. The calculation result for the system is not sensitive with respect to these parameters.

A special emphasis is needed not the phase separation inside the slightly inclined heat transfer tubes. Although the basic formalism is based on the drift flux model, the formalism is used in a modified way. The liquid velocity downwards in the existence of steam is calculated from the shear and gravitational balance, where for the liquid the shear with gas and tube wall is defined, and the difference is defined as the gravitational effect. But the model is applied only for the stratified flow conditions. The stratification criteria is based on the Tandon's flow regime map. Tandons flow regime map (Tandon, 1983) was recommended by (Schaffrath, 2001) in their analyses of condensation in horizontal tubes. They conclude that Tandons flow regime map is one of the newest flow maps for condensation inside horizontal tubes and it agrees excellently in annular and stratified flows with data of other researchers. The map is based on the Wallis dimensionless steam velocity j^*_g, which is defined as

$$j_g^* = \frac{xG_g}{\sqrt{gD(\rho_l - \rho_g)}} \tag{36}$$

where x = gas mass fraction, G = total mass flux, kg/s/m^2 , D = tube diameter.

Tandon defined the boundaries between the different flow regime maps, table 2.

Table 2 Boundaries of flow regimes in Tandons flow map.

stratified	$j^*_g < 1$	and	$(1-\alpha)/\alpha < 0.5$
annular	$1 < j^*_g < 6$	and	$(1-\alpha)/\alpha < 0.5$
spray	$j^*_g > 6$	and	$(1-\alpha)/\alpha < 0.5$
bubble	$j^*_g > 0.5$	and	$(1-\alpha)/\alpha > 0.5$
slug	$0.01 < j^*_g < 0.5$	and	$(1-\alpha)/\alpha > 0.5$
plug	$j^*_g < 0.01$	and	$(1-\alpha)/\alpha > 0.5$

Thus the criteria $j^*_g < 1$ is applied as the criteria together with $(1-\alpha)/\alpha < 0.5$ for simulating the liquid film flow with the shear model. After film flow is defined, the gas velocity may be calculated from the total mixture flow.

3.3 Heat transfer in the condensing horizontal tubes

The heat transfer from the tube inside to the shell side includes three phases, and the total heat transfer is defined through, where the heat transfer from gas to liquid, liquid to wall, through the wall, and on the shell side are differentiated and the effective heat transfer coefficient is derived for the heat transfer chain as.

$$q'' = \frac{T_{in} - T_{out}}{\frac{1}{h_{in}} + \frac{l_w}{\lambda_w} + \frac{l_{tube}}{\lambda_{tube}} + \frac{1}{h_{out}}} \quad (37)$$

In the condenser is assumed as a film over the wall. The thickness is defined from the local mass, and the heat transfer chain is solved for defining the film inside temperature.

In the stratified flow regime the wall surface above the water level is assumed condensing steam in the film-wise mode. The heat flux downwards is calculated through the water layer on the bottom of the tube. The key question is the condensation heat transfer between steam and subcooled liquid.

The condensation heat transfer coefficient in accordance with the Nusselts theory for the laminar film is given through

$$h_f = 1.1025\,\lambda_l\,\mathrm{Re}_f^{-0.33}\left(\frac{\rho_f(\rho_f-\rho_g)g}{\mu_l^{\,2}}\right)^{0..33} \quad (38)$$

In the steam generator the single phase forced convection heat transfer of Dittus-Boelter is applied.

4. NUMERICAL SOLUTION OF THE 3-D TWO-PHASE MIXTURE EQUATIONS

The selected discretization grid for the 2-D model of the experimental facility is illustrated in Figure 4 for the Cartesian coordinates.

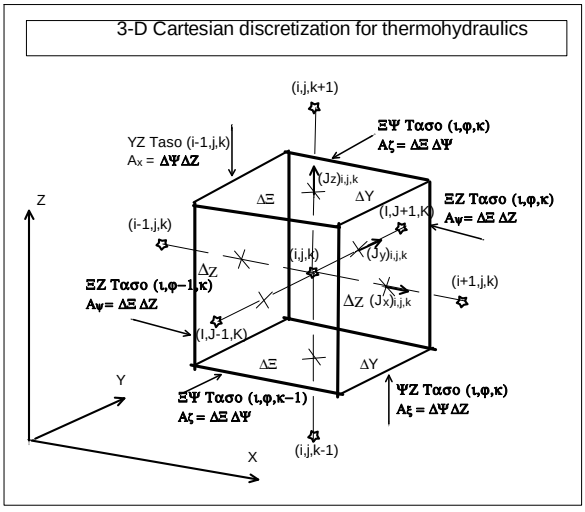

Figure 4. Numerical scheme in the solution of the three-dimensional two-phase flow equation in Cartesian coordinates.

The "i" – and "j" indexes are used in the horizontal direction and "k" –index in the vertical direction. The state variables, temperatures, pressure, enthalpies, void fraction, phase mass, heat capacity, heat conductivity over the cell and all heat transfer quantities are attached to the mesh cell center points. The flow and flux variable are attached to cell boundaries and the vertical direction and horizontal direction are separated from each other. The flow variables include the mass flow rates, velocities and volumetric flow rates. The flux variable include the conduction heat flux between mesh cells. The indexing of cell boundaries is shown in Figure 6. The "next" boundary in the vertical and horizontal direction has the same index as the center point has. In addition to the traditional (i,j) indexing the notation used in the numerical solutions of matrices are pointed out. These notations are identified through cardinal points

The numerical solution of discretized equations is based on the ADI (altering-direction-implicit) method where for all x-, y- and z-direction diagonals alternately the new pressure guess is solved and the solution is repeated so many times the iteration converges. For the geometries with less than 30000 mesh points the direct sparse matrix inversion is used optionally.

The ADI method is used for the void fraction and enthalpy solutions as well, but for these iterations only two sweeps are used systematically. The original matrix set-up for the pressure velocity iteration is weakly diagonal dominant, and that is why the convergence is difficult for this matrix inversion.

The void fraction and enthalpy equations include a significant diagonally dominance and the equations are formulated using semi-implicit donor-cell discretization that even in the case having iteration not fully converged, the solutions have a self-stabilising character.

The essential feature in the numerical solution is that the enthalpy equations (9) and (10) are solved separately, because the enthalpies are loosely coupled together and to the flow dynamic equations. Inside the water pool steam is practically saturated, but its solution is included into the model for other possible code applications.

The mass and momentum conservation are coupled together through the discretized equation for all directions as

$$\begin{aligned}&\frac{\varepsilon V_{ij}}{\Delta t}\left(\frac{\alpha}{\rho_g}\frac{\partial \rho_g}{\partial p}+\frac{1-\alpha}{\rho_l}\frac{\partial \rho_l}{\partial p}\right)\left(p^*_{i,j,k}-p_{i,j,k}\right)+\\ &\left((J_{mz})_{i,j,k}-(J_{mz})_{i,j-1,k}\right)^*+\left((J_{mr})_{i,j,k}-(J_{mr})_{i-1,j,k}\right)^* \quad (39)\\ &+\left((J_{mr})_{i,j,k}-(J_{mr})_{i-1,j,k}\right)^*=\Gamma_{i,j,k}\left(\frac{1}{\rho_g}-\frac{1}{\rho_l}\right)\end{aligned}$$

derived from the mass conservation equation and the momentum equations written for different coordinate directions.

The effect of the phase separation may be solved outside the pressure solution, which is directly giving the volumetric flow components in different directions in an arithmetic form.

The void fraction has to be predicted for the new by using the equation

$$\begin{aligned}&\alpha^{n+1}_{i,j,k}\rho^{n+1}_{g,i,j,k}V_{i,j,k}=\alpha^{n}_{i,j,k}\rho^{n+1}_{g,i,j,k}V_{,j,ki}+\\ &\sum_{\substack{ix=i-1\\ixx=i-1}}^{i+1}{}^{i}<J^{n+1}_{g,ix,j,k},0>\alpha^{n+1}_{ixx,j,k}V_{i,j,k}+\\ &\sum_{\substack{jx=j-1\\jxx=j-1}}^{j+1}{}^{j}<J^{n+1}_{g,i,jx,k},0>\alpha^{n+1}_{i,jxx,k}V_{i,j,k}+\\ &\sum_{\substack{kx=k-1\\kxx=k-1}}^{k+1}{}^{k}<J^{n+1}_{g,i,j,kx},0>\alpha^{n+1}_{i,j,kxx}V_{i,j,k}+\Gamma^{n+1}_{g,i,j,k}\Delta t\end{aligned} \quad (40)$$

The void fraction in the node depends on the neighbouring nodes as well. After solving the phase separation the mass flow rates may be calculated

The energy equations may be solved outside the volumetric flow and mass flow equations.

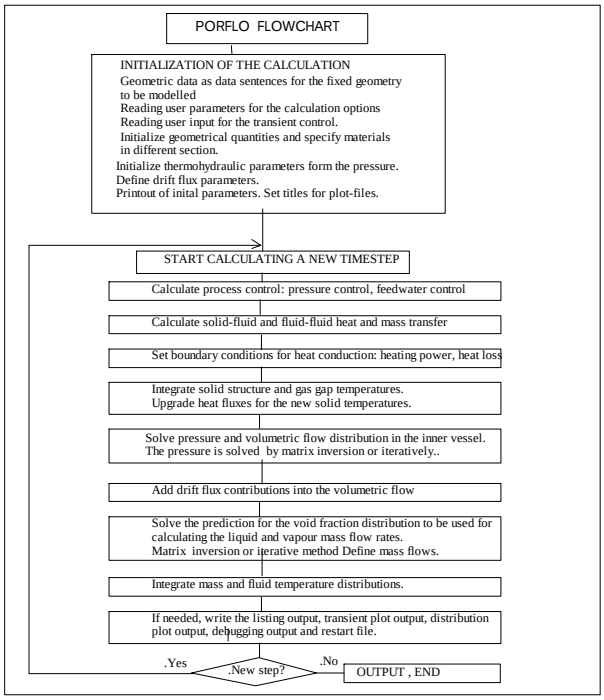

Figure 5. Solution structure in the PORFLO code.

The solution in PORFLO is organised as shown in Fig.5.

5. SIMULATION OF THE ISOLATION CONDENSER

In the first applications the cylindrical pool was modelled as a rectangular volume having equivalent dimensions. The model contains 10260 grid points. The heat transfer tubes are described with porous area with 8·7·8 grid, figure 6.

The initial temperature of the pool was 90 °C and pressure was 2 bar. A constant heat generation of 100 MW was set to heat exchanger tube area.

Fig. 7 shows that the simulated void fraction and temperature distribution in the cut j=4 at 95 s. The pool has started to heat up, but water is saturated only in the tube bundle area. Saturation temperature in this area is about 120 °C. There is vigorous boiling in the tube bundle area, but it is surrounded by subcooled water and bubbles rising from the tube bundle condense almost immediately. This fast condensation needs further analyses, since condensation efficiency depends, among other things, on bubble size. The possible bubble sizes have to be evaluated and their effect on condensation has to be analysed with varying model parameters and correlation.

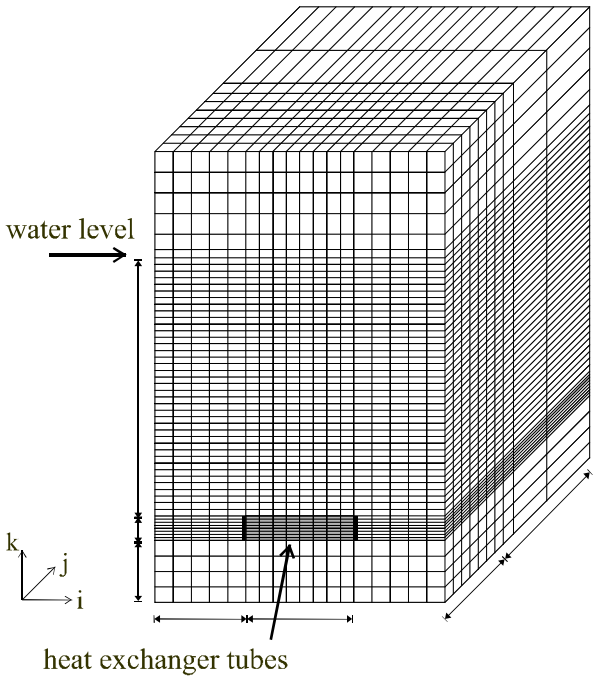

Figure 6. Model of IC pool in the simulations with PORFLO.

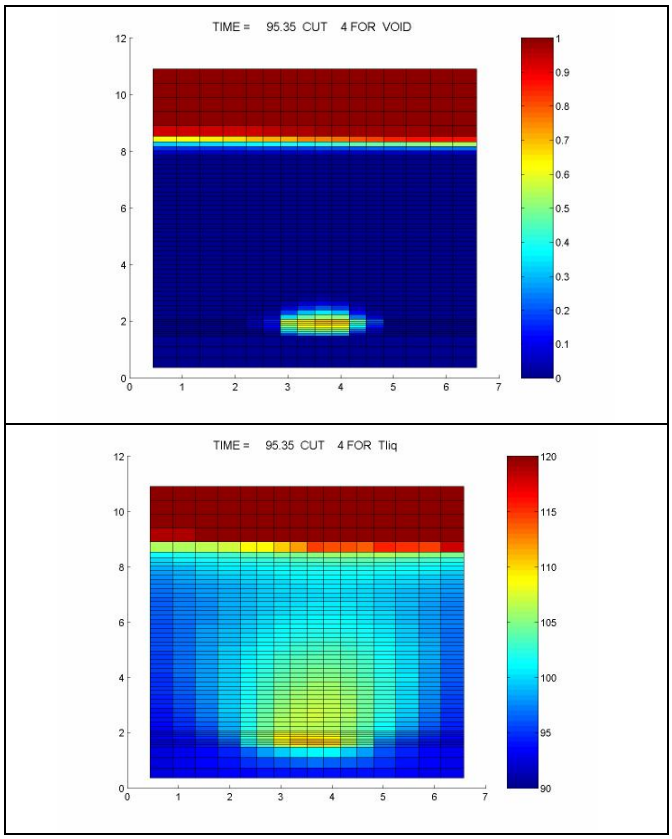

Figure 7. Pool void fraction and temperature distribution in PORFLO simulation.

CONCLUSIONS

The porous media model PORFLO is under development at VTT for diverse multidimensional flow applications.

The first applications were related to the STYX experiments for the dryout of the internally heated particle bed, simulating the coolability of the corium released from the BWR reactor to the water pool in the containment floor. The analyses are still in progress and more final conclusions can be drawn after comparing against other analytical tools .

As a second application the model was used for two-phase flows in pools, where strong circulation is created by the evaporation caused by the released from the condensing steam flow inside the tube bundle. The model allows more detailed modelling for the condensing heat transfer inside the horizontal tubes as well.

In the analysis of the horizontal steam generator is one of future applications. In this case the solution for the single phase liquid flow solution inside the primary tubes is included into the model as a boiling heat source for the secondary side.

The development of the PORFLO model demonstrates needs for understanding the multidimensional two-phase flow in the large process facilities. In the first phase the solution based on a drift-flux model has makes the solution rather stable with respect to the pressure and volumetric flow distribution and with respect to the phase separation. The solution of the pressure distribution together with the volumetric flow distribution is most challenging solution in this formalism, but the matrix inversion methods of the single phase multidimensional flow may be applied for this matrix inversion as well. The formulation of equations for the full two-fluid solution is much more complex.

NOMENCLATURE

A	Flow or surface area, m^2
C	Concentration, coefficient
D	Diameter, m
f	Friction factor
g	Acceleration of gravity , 9.81 ms^{-2}
G	Total mass flux, kg s^{-1} m^{-2}
h	Heat transfer coefficient, $Wm^{-3}K^{-1}$
h	Enthalpy, $kJkg^{-1}$
j	Superficial velocity, ms^{-1}
j_g^*	Wallis dimensionless gas velocity, -
J	Volumetric flow, m^3 s^{-1}
Nu	Nusselt Number (hD/k), -
p	Pressure, Pa
q''	Heat flux, W/m^2K
q'''	Heat flux, W/m^3K
T	Temperature, K, ^oC
u, v and w, x-, y-, z-velocity, ms^{-1}	
V	Volume, m^3
V_{gj}	Drift flux velocity, m/s
x, y and z, Cartesian coordinate, m	

Greek symbols

α	Volume fraction of gas phase, -
ε	Porosity (=fluid volume per total volume)
γ	Vapour generation rate, $kgm^{-3}s^{-1}$
μ	Dynamic viscosity, Pa*s
λ	Thermal conductivity, W/mK
ρ	Density, kgm^{-3}
σ	Surface tension of liquid, kg s^{-2}

Subscripts

b	boiling
CHF	critical heat flux
con	condensation
eq	equivalent
lg	evaporation
fla	flashing
fl	fluid
fric	friction
g	gas phase (vapour)
h	heated
l	liquid phase
m	mixture
s	saturation
w	wall

REFERENCES

Dowlati R., Chan A.M.C., Kawaji M., 1992, Hydrodynamics of Two-Phase Flow Across Horizontal In-line and Staggered Rod Bundles, Transactions of the ASME, Vol 114, September 1992, pp. 450-456.

Ferng Y-M., Ma Y-P., Kang J-C., 2001, Thermal Hydraulic Simulation of Localized Flow Characteristics in a Steam Generator, Nuclear Technology, Vol 136, Nov. 2001, pp.186-196.

Haukeland S., Ivung B. and Pedersen T., 2000, BWR 90+: A Competitive Nuclear Power Alternative, PowerGenEurope 2000, Helsinki, Finland

Miettinen J., Sairanen R., Holmström S., Lindholm I., 2000, Experimental Study and Analytical Methods for Particle Bed Dryout With Heterogeneous Particles and Pressure Variation, ICONE-8, April 2-6, 2000, ICONE-22420, Baltimore, MD USA.

Schaffrath A., Hicken E.F., Jaegers H., Plasser H.M., 1999, Experimental and Analytical Investigation of the Operation Mode of the Emergency Condenser of the SWR 1000, Nuclear Technology, Vol 126, (1999) p. 123-141

Schaffrath A., Krüssenberg A.-K., Fjodorow A., Gocht U., Lischke W., 2001, Modeling of condensation in horizontal tubes, Nuclear Engineering and Design 204 (2001) p. 251-265.

Tong L.S., 1972, Boiling Crisis and Critical heat Flux, AEC Critical Review Series, 1972, 82 p.

Tandon, T.N., Varma H.K., Gupta C.P.,1982, A New Flow Regime Map for Condensation Inside Horizontal Tubes, Journal of Heat Transfer, Nowember 1982, Vol. 104, p. 763-76